


# Sinomenine Inhibits Orthodontic Tooth Movement and Root Resorption in Rats and Enhances Osteogenic Differentiation of PDLSCs

Hongkun Li , Yilin Li, Jinghua Zou, Yanran Yang, Ruiqi Han, Jun Zhang

Shandong University & Shandong Key Laboratory of Oral Tissue Regeneration & Shandong Engineering Laboratory for Dental Materials and Oral Tissue Regeneration, Department of Orthodontics, School and Hospital of Stomatology, Cheeloo College of Medicine, Shandong University, Jinan, People's Republic of China

Correspondence: Jun Zhang, Shandong University & Shandong Key Laboratory of Oral Tissue Regeneration & Shandong Engineering Laboratory for Dental Materials and Oral Tissue Regeneration, Department of Orthodontics, School and Hospital of Stomatology, Cheeloo College of Medicine, Shandong University, No. 44-1 Wenhua Road West, Jinan, 250012, People's Republic of China, Tel +86 139 5310 9816, Email zhangj@sdu.edu.cn

**Purpose:** To investigate the effects of sinomenine on orthodontic tooth movement and root resorption in rats, as well as the effect of sinomenine on the osteogenesis of periodontal ligament stem cells (PDLSCs).

**Methods:** Fifty-four male Wistar rats were randomly divided into 3 groups: control group, 20 mg/kg sinomenine group and 40 mg/kg sinomenine group. Fifty-gram orthodontic force was applied to all groups. Each group was injected intraperitoneally with corresponding concentration of sinomenine every day. After 14 days, all rats were sacrificed. Micro-computed tomography (micro-CT) scan was used to analyze tooth movement, root resorption and alveolar bone changes. The effect on periodontal tissue was analyzed by Masson, tartrate-resistant acid phosphatase (TRAP) and immunohistochemical staining. In vitro, PDLSCs were extracted and identified. The effect of sinomenine on proliferation was determined by cell-counting kit-8. The effect of sinomenine on osteogenesis was investigated by alkaline phosphatase (ALP) activity and alizarin red staining. qPCR and Western blotting were performed to explore the effects of sinomenine on the expression levels of ALP, runt-related transcription factor 2 (RUNX2), receptor activator of nuclear factor kappaB ligand (RANKL) and osteoprotegerin (OPG).

**Results:** The tooth movement and root resorption of sinomenine groups were reduced. Sinomenine decreased trabecular spacing on compression side and increased alveolar bone volume and trabecular thickness on tension side. TRAP-positive cells in sinomenine groups decreased significantly. The expressions of TNF- $\alpha$  and RANKL were decreased, while the expressions of OPG, RUNX2 and osteocalcin were up-regulated. In vitro, 0.1 M and 0.5 M sinomenine enhanced ALP activity, mineral deposition and the expression of ALP, RUNX2 and OPG, and reduced the expression of RANKL.

**Conclusion:** Sinomenine could inhibit tooth movement, reduce root resorption, and exert a positive effect on bone formation in rats. Moreover, sinomenine promoted the osteogenesis of PDLSCs.

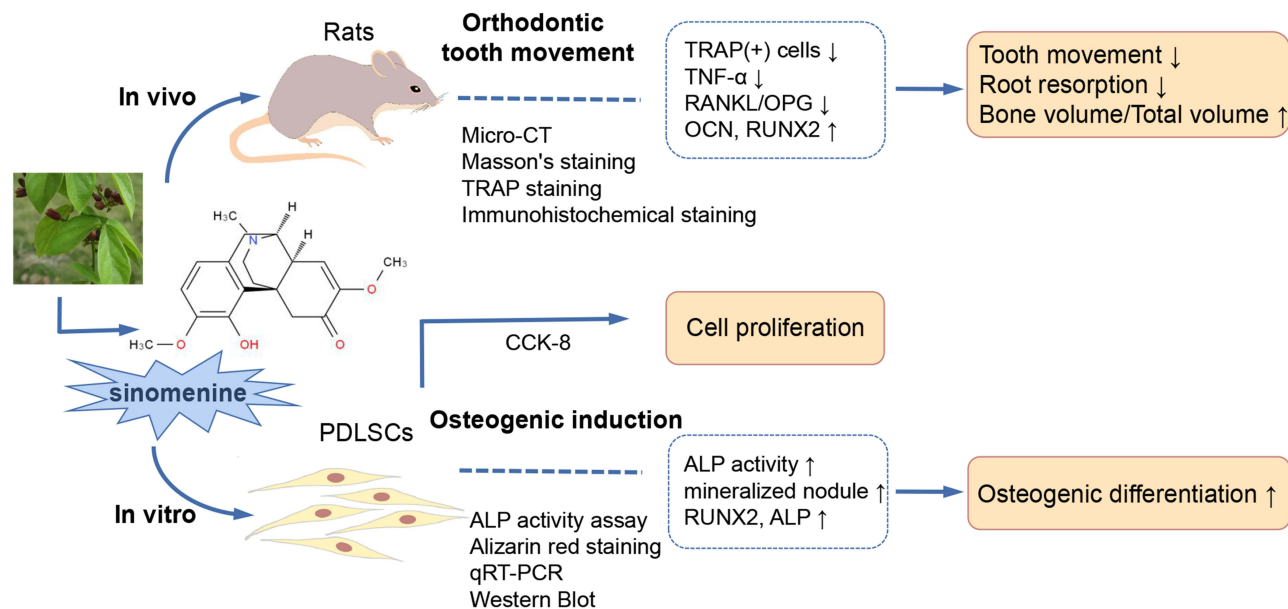
**Keywords:** sinomenine, tooth movement, root resorption, osteoclast, osteogenesis

## Introduction

Orthodontic tooth movement (OTM) during orthodontic treatment is based on the remodeling of periodontal tissue. Under the action of mechanical force, the dynamic balance between bone formation and resorption of periodontal tissue is disturbed. Alveolar bone at the tension side undergoes bone formation, and bone resorption occurs at the compression zone.<sup>1</sup> The remodeling speed of periodontal tissue is a key factor affecting the speed of OTM. The process involves the communication and regulation among a variety of cells, among which osteoclast-mediated bone resorption and osteoblast-mediated bone formation are tightly coupled processes regulated by various cytokines, chemokines and their receptors and other inflammatory mediators.

Receptor activator of NF-kappaB (NK- $\kappa$ B) ligand (RANKL) is a critical cytokine for osteoclastogenesis as a membrane associated cytokine.<sup>2</sup> Osteocytes, osteoblasts and stromal cells express RANKL stimulated by bone

## Graphical Abstract



resorption factors. Osteoclast precursor cells express RANK, which is a receptor for RANKL. Binding of RANKL to RANK initiates multiple downstream signal transduction pathways and then induces osteoclastic differentiation.<sup>3,4</sup> In addition, osteoblasts and stromal cells produce osteoprotegerin (OPG), which is a decoy receptor for RANKL. OPG can inhibit the interaction between RANKL and RANK, so as to inhibit osteoclast differentiation and bone resorption.<sup>5</sup> Enhancing RANKL gene expression through local RANKL gene transfection can significantly enhance bone resorption, improve the rate of bone remodeling and promote OTM.<sup>6</sup> Correspondingly, local OPG gene transfection can inhibit bone resorption and inhibit OTM.<sup>7</sup> In contrast, severe RANKL genetic defects can lead to a special form of autosomal recessive osteopetrosis (ARO), which is characterized by bone resorption failure of osteoclasts, resulting in increased bone mineral density.<sup>8–10</sup> OPG-deficient mice have been shown to exhibit severe osteopetrosis and difficulty in tooth eruption, accompanied by the complete lack of osteoclasts due to the inability of osteoblasts to induce the formation of osteoclasts.<sup>11</sup>

Periodontal ligament is a soft, fibrous connective tissue, which is embedded between cementum and the inner wall of alveolar bone. Periodontal ligament stem cells (PDLSCs) can be isolated from periodontal ligament tissue.<sup>12</sup> They have high self-renewal ability and multilineage differentiation potential. PDLSCs play a vital role in maintaining periodontal homeostasis.<sup>12</sup> Under appropriate induction conditions, PDLSCs can differentiate into different cell lineages, such as osteoblast-like cells, cementoblast-like cells, adipocytes and fibroblast-like cells.<sup>13,14</sup> In vivo studies have found that PDLSCs can promote the damaged periodontal tissue to form new alveolar bone tissue, periodontal ligament and cementum.<sup>15–17</sup> It has been reported that PDLSCs are the most promising differentiation source for alveolar bone regeneration.<sup>18</sup> In conclusion, PDLSCs are considered to have a broad application prospects in the field of periodontal tissue regeneration engineering. In addition, PDLSCs plays an extremely important role in the remodeling of periodontal ligament and alveolar bone during orthodontic tooth movement.<sup>19</sup> Zhang established OTM rat model and tracked the response of PDLSCs in vivo.<sup>20</sup> The study found that PDLSCs on both compression and tension sides could be reactivated during orthodontic treatment.<sup>20</sup> PDLSCs also participate in the relapse process after orthodontic treatment.<sup>21</sup> In vitro studies found that mechanical stress could promote the osteogenic differentiation and proliferation of PDLSCs.<sup>20,22</sup> Generally, PDLSCs play an important role in OTM, which may involve a variety of mechanoreceptors and pathways, such as cytoskeleton, MAPK signal, TGF-β/Smad, Wnt/β-Catenin pathway and RANKL/OPG axis.<sup>20,21,23–25</sup>

Sinomenine (SIN), a natural alkaloid, is the main component of the traditional Chinese medicine *sinomenium acutum*. Sinomenine is known for its obvious therapeutic effects, such as anti-inflammatory, immunosuppressive, antioxidant, antiarrhythmic and anti-cancer.<sup>26–33</sup> It is widely used in the clinical treatment of rheumatoid diseases. In addition, some studies have found that sinomenine has an effect on bone metabolism.<sup>34–36</sup> It has been reported that sinomenine can inhibit the differentiation of osteoclasts via RANKL signaling pathways.<sup>36</sup> In addition, sinomenine could promote the differentiation of osteoblasts by regulating the Akt/RUNX2 signaling pathway.<sup>34</sup> It is reported that sinomenine may increase the expression of osteogenic markers such as ALP, OCN, type I collagen (COL1A1) and osteopontin in MC3T3-E1 cells.<sup>34</sup>

Based on previous studies, we proposed the hypothesis that sinomenine might inhibit OTM and root resorption in rats and promote osteogenic differentiation of PDLSCs. To the best of our knowledge, there is no *in vivo* or *in vitro* study related to the effect of sinomenine on OTM and PDLSCs osteogenesis. Therefore, in this study, we explored the effect of sinomenine on OTM and orthodontic induced root resorption (OIRR) in rats and investigated the effect of sinomenine on the osteogenesis of PDLSCs. We anticipate that the results of this study will provide a valuable reference for the clinical effect of sinomenine on orthodontic treatment and the application of sinomenine in periodontal tissue regeneration engineering.

## Materials and Methods

### Animal Experiment

#### Animals and Groups

The animal experiment in this study was approved by the Institutional Animal Ethics Committee of Shandong University (No.20220104) and was performed according to the ARRIVE guidelines.<sup>37</sup> Fifty-four 6-week-old male Wistar rats weighing  $180 \pm 15$  g were purchased from SPF biotechnology company (Beijing, China) and maintained in accordance with the guidelines of the institutional ethics committee of Shandong University. The rats were pair-housed in standard plastic cages under specific pathogen-free conditions. They were raised under constant environmental conditions of room temperature ( $21 \pm 1$  °C),  $55 \pm 10\%$  relative humidity and a 12-hour light/dark cycle. The interior noise was below 60 dB. Ensure nutrition through laboratory powder diet and water *ad libitum*. All animals had been adapted for 1 week before the experiment began. During the experiment, the general condition and body weight of each animal were monitored.

The rats were randomly divided into 3 groups ( $n = 18$  per group): (1) control group (normal saline); (2) low-dose sinomenine treatment group (20 mg/kg sinomenine); (3) high-dose sinomenine treatment group (40 mg/kg sinomenine). Dissolve sinomenine (Solarbio, Beijing, China) in 0.05% dimethyl sulfoxide to prepare the stock solution. The stock solution was diluted to the required concentrations with an appropriate amount of normal saline immediately before use. Rats in the low-dose and high-dose groups were intraperitoneally injected with sinomenine at a dose of 20 mg/kg/d and 40 mg/kg/d. Rats in the control group were intraperitoneally injected with normal saline for 14 days.

#### Animal Model and Study Design

All rats received orthodontic treatment (Figure 1A). After isoflurane (Yipin Pharmaceutical Co., Ltd, Hebei, China) inhalation anesthesia, 3% phenobarbital sodium was injected intraperitoneally at a dose of 35mg/kg. After anesthesia, a 0.5 mm groove was prepared around the neck of the two maxillary incisors. A 0.2 mm stainless steel wire (Aosu Medical Instrument Co., Ltd, Hangzhou, China) was placed on the right maxillary first molar. Then, a nickel–titanium (Ni-Ti) closed-coil spring (Grimed Medical Co., Ltd, Beijing, China) was inserted between the right maxillary first molar and incisors producing a 50 g orthodontic force verified by an ergometer (Westlake Biomaterial, Hangzhou, China) to move the right first molar. The proximal end of the closed-coil spring was fixed on the incisor neck through stainless steel wire embedded in the groove of the incisor and reinforced with light-curing resin to strengthen anchorage and reduce the movement of incisors. During the experiment, each rat was checked every day to ensure the integrity of the device.

After 14 days of tooth movement, all rats were injected with sodium pentobarbital intraperitoneally at a dose of 200 mg/kg for anesthesia.<sup>38</sup> The rats then perfused fixation by cardiac puncture with 4% paraformaldehyde (pH = 7.4). The maxilla of the experimental subjects containing the right maxillary molar was dissected and trimmed, and then the obtained specimens were fixed in 4% paraformaldehyde solution for 24 hours. During this period, the samples were

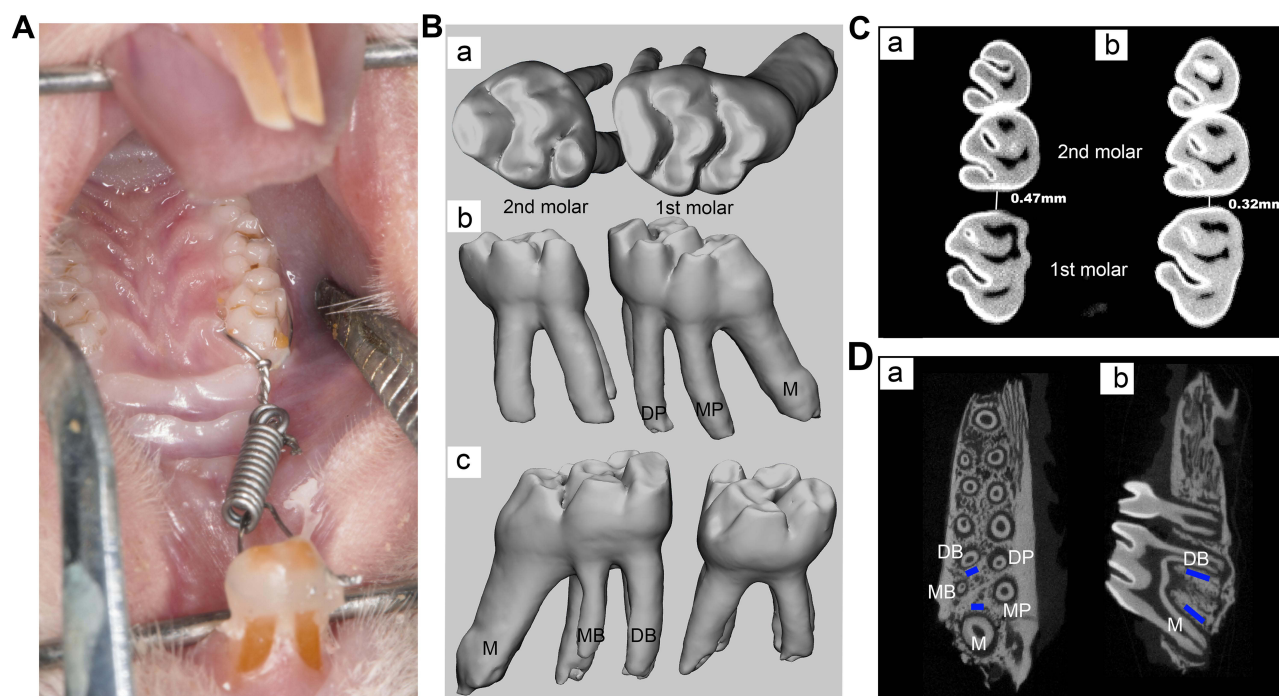


**Figure 1** Model of orthodontic treatment and analysis of micro-CT. **(A)** Rat model of orthodontic treatment. **(B)** 3D images of the right maxillary first and second molars. a, occlusal view; b, palatal view; c, buccal view. **(C)** Tooth movement measurement of right maxillary first molar: a, control group; b, high-dose sinomenine group. **(D)** Region of interest (ROI) of bone analysis is marked in blue. a, horizontal view; b, vertical view.

**Abbreviations:** M, mesial root; MB, midbuccal; DB, distobuccal; MP, mesiopalatal; DP, distopalatal.

scanned by micro-computer tomography (micro-CT) scanner. The specimens were then decalcified in 10% ethylenediaminetetraacetic acid (EDTA) at 4 °C for two months. The solution was changed 3 times a week. Thereafter, the specimens were washed by current water, dehydrated by graded ethanol, cleared in xylene and embedded in paraffin. The sample was cut into 5 µm thickness slices by a microtome (Leica, RM 2035, Germany) in a direction parallel to the long axis of the distopalatal root. The sections then performed Masson staining, Tartrate-resistant acid phosphatase (TRAP) staining and immunohistochemical analysis.

### Micro-Computed Tomography (Micro-CT)

As mentioned above, the specimens on day 14 were scanned with micro-CT scanner (Quantum GX2 micro-CT, PerKinElmer, USA). The scanning condition was 90 kV, 88 µA. The layer thickness was 36 µm, and each scanning time was 14 min. The raw image was reconstructed and converted into DICOM format using the built-in software. The 3D images of maxillary first and second molars were extracted by Mimics 21.0 (Figure 1B). According to previous study, the distance between the contact points of the right maxillary first and second molar was measured on a two-dimensional cross-section as the amount of OTM (Figure 1C).<sup>39</sup> Then, the extracted 3D model was imported into Geomagic Studio 2014 software (Geomagic Inc., NC, USA), and the volume of the first molar was measured. After repairing the root resorption zone by Geomagic Studio to form the smooth continuous state, the volume was remeasured and the difference between the two volumes was calculated as the root resorption volume. Micro-CT images were analyzed by a CT-Analyser (CTAn; Skyscan NV). Two regions of interest (ROI, Figure 1D) with the volume of 200 × 400 × 800 µm were selected at the proximal alveolar bone of the distobuccal root and the distal alveolar bone of the mesial root of the first molars. The following microstructure parameters were measured: bone volume/total volume (BV/TV), trabecular thickness (Tb.Th) and trabecular separation/spacing (Tb.Sp).

### Histological and Immunochemical Analysis

Sections were dried at 60 °C for 2 h and then deparaffinized in xylene for 20 minutes. Then, the slides were hydrolyzed with a series of gradient ethanol and rinsed in ddH<sub>2</sub>O. The processed slices were stained as follows. (1) The sections



were stained with a Masson's trichrome staining kit (Servicebio, Hubei, China) according to the manufacturer's instruction. In Masson's trichrome staining, collagen fibers and new bone were dyed blue. (2) The sections performed TRAP staining by a TRAP staining kit (Solarbio, Beijing, China) to identify clastic activity at the mesial side of distopalatal root of the right maxillary first molar. The polynuclear TRAP-positive cells around the alveolar bone were considered as osteoclasts, while the positive cells on the root surface were considered as odontoclasts as previously mentioned.<sup>40</sup> The number of TRAP-positive cells at mesial side of distopalatal root was counted. In addition, the quantitative evaluation of TRAP-positive cells was further performed by analyzing the number of TRAP-positive cells on the mesial side of the distopalatal root/the distopalatal root area (dentine and pulp) within the same slice. (3) For immunohistochemical staining, the sections were incubated in 3% hydrogen peroxidase in formaldehyde for 15 minutes to reduce the nonspecific staining caused by endogenous peroxidase. Subsequently, slices were incubated on ice with goat serum for 40 minutes. Polyclonal anti-rabbit TNF- $\alpha$  (1:300; Servicebio, Hubei, China), RANKL (1:300; Solarbio, Beijing, China), OPG (1:50; Solarbio, Beijing, China), RUNX2 (1:400; Solarbio, Beijing, China) and osteocalcin (OCN, 1:400; Solarbio, Beijing, China) as primary antibodies were incubated overnight at 4 °C. A rabbit anti-goat immunoglobulin was applied as secondary antibody and incubated for 30 minutes. After washing, the slides were processed with biotin-streptavidin horseradish peroxidase (HRP) detection system by an SP Kit (Solarbio, Beijing, China). The sections were observed under the microscope after slight counterstaining with haematoxylin solution.

## Cell Experiment

### Isolation and Cultivation of PDLSCs

The study was conducted in accordance with the Declaration of Helsinki. The collection and usage of PDLSCs were approved by the Ethics Committee of Shandong University (No.20220103). The written informed consent of all patients (or children's legal guardians) has been obtained. As previously reported, PDLSCs were isolated and cultured.<sup>41</sup> Twenty non-carious premolars completely extracted due to orthodontics (patients' age: 16–24 years old) were collected and stored in a precooling  $\alpha$ -minimum essential medium ( $\alpha$ -MEM; Hyclone, Logan, UT, USA) containing 5% penicillin/streptomycin antibiotics (Sigma-Aldrich, St. Louis, MO, USA) immediately, and the extraction of PDLSCs was completed within 4 h. Teeth were rinsed with phosphate buffered saline (PBS) containing 5% penicillin/streptomycin. Then, the periodontal ligament in the middle third of the root was scraped with a sterile blade and cut into small pieces. These small tissue blocks were transferred into the bottom of a cell culture flask. After adding  $\alpha$ -MEM containing 20% fetal bovine serum (FBS; BioInd, Kibbutz, Beit-Haemek, Israel) and 1% antibiotics, the cell culture flask was erected in 37 °C, 5% CO<sub>2</sub> incubator and turned over after 4 h. The culture medium was renewed every three days and replaced with  $\alpha$ -MEM supplemented with 10% FBS after the appearance of cells. The spindle shape of PDLSCs was observed under the microscope. The obtained cells were isolated and purified by limited dilution cloning method. The primary cells were prepared into a single-cell suspension and diluted to 10 cells/mL. Individual cells were seeded into 96-well plates. After 12 hours of culture, single-cell wells were marked and the culture was continued. All single-cell clones were collected to obtain purified PDLSCs. PDLSCs from P3-P5 were used in subsequent experiments.

### Characterization and Multidirectional Differentiation of PDLSCs

The cells were isolated via treatment with 0.25% trypsin-EDTA (Thermo Fisher Scientific Inc., Waltham, MA, USA), and the dispersed cells were washed with PBS. The expression of cell surface markers CD34, CD45, CD90 and CD105 (eBioscience, San Diego, CA, USA) were analyzed by flow cytometer (Beckman Coulter, Brea, CA, USA). The multidirectional differentiation ability of PDLSCs was detected by inducing osteogenic and adipogenic differentiation. The cells were plated in 6-well plates at a density of  $1.5 \times 10^5$  cells per well. After culturing in the complete medium for 24 h, the medium was replaced with osteogenic induction medium ( $\alpha$ -MEM containing 10% FBS, 10 mM  $\beta$ -glycerophosphate, 50 mg/L ascorbic acid, and 1  $\mu$ M dexamethasone) or adipogenic inducing medium ( $\alpha$ -MEM containing 10% FBS, 1  $\mu$ M dexamethasone, 10  $\mu$ g/mL insulin, 0.2 mM indomethacin and 0.5 mM 3-isobutyl-1-methylxanthine).

The culture medium was changed every 3 days. After 21 days in dark, PDLSCs were stained with Alizarin Red S and oil red O (Solarbio, Beijing, China) and observed under the microscope.

### Cell Proliferation Was Detected by CCK-8 Kit

The effects of sinomenine on the proliferation of PDLSCs were determined by Cell Counting Kit-8 (CCK-8; Dojindo Laboratories, Kumamoto, Japan). PDLSCs were plated in 96-well plates at a density of  $3 \times 10^3$  cells per well. After the cell cultured in complete medium for 24 h, the medium was replaced by complete medium supplemented with 0, 0.1, 0.2, 0.5, 1.0 or 2.0 M sinomenine (Solarbio, Beijing, China) for 24, 48, and 72 hours. The cell-free group was set as the blank control. Five replicates were performed for each group. After aspirating the medium, CCK-8 was added according to the instruction ( $\alpha$ -MEM and CCK-8 reagent were mixed at a 9:1 ratio), and the absorbance was measured at 450 nm after incubation at 37 °C in a darkroom for 2 h on a microplate reader (SPECTRAstar Nano, BMG Labtech, Ortenberg, Germany).

### Alkaline Phosphatase Activity Assays and Alizarin Red S Staining

The cells were plated in 6-well dishes as above, and the culture medium was changed into osteogenic induction medium containing 0, 0.1 and 0.5 M sinomenine after 24 h. After 7 days of incubation, whole-cell protein extracts were obtained using RIPA Lysis Buffer (Beyotime, Shanghai, China) containing 1% PMSF (Beyotime, Shanghai, China). The collected lysate was centrifuged (4 °C, 12,000  $\times$  g, 5min) after ultrasonic lysis, and then the supernatant was collected. The protein concentration was detected by a BCA protein assay kit (Solarbio, Beijing, China). In order to reduce proteinase activity, the operation process was carried out on ice. Alkaline phosphatase (ALP) activity was quantitatively analyzed by an alkaline phosphatase test kit (Nanjing Jiancheng Bioengineering Institute, Nanjing, China). The absorbance of the sample was measured at a wavelength of 520 nm by a microplate reader.

After 21 days of induction, alizarin red staining was performed and the stained plates were observed and photographed under the microscope. Thereafter, 10% cetylpyridinium chloride (CPC; Solarbio, Beijing, China) was used to dissolve mineralized nodules, and the absorbance of the solution at 562 nm wavelength was measured to quantify mineralized matrix formation.

### RNA Isolation and Quantitative Real-Time PCR

After 7 days of culture, total RNA was extracted with Trizol (TaKaRa, Shiga, Japan) and reverse transcribed into cDNA using a Primer Script<sup>®</sup> RT Reagent Kit (TaKaRa, Japan). SYBR<sup>®</sup> Premix Ex Taq<sup>™</sup> (TaKaRa, Japan) and a Roche Light Cycler<sup>®</sup> 96 Sequence Detection System (Roche Diagnostics GmbH, Mannheim, Germany) were used for quantitative real-time PCR (qRT-PCR). Relative gene expression was measured by comparative  $2^{-\Delta\Delta C_t}$  method<sup>42</sup> for ALP, RUNX Family Transcription Factor 2 (RUNX2), OPG and RANKL. Each sample was assayed in triplicate. The primer sequences for the qRT-PCR are shown in [Supplementary Table 1](#).

### Protein Detection via Western Blot

After 7 days of culture, the cells were lysed, the proteins were collected, and the total protein concentration was detected by a BCA protein assay kit. The expression levels of ALP, RUNX2, OPG and RANKL were determined by Western blot. The protein was separated by 10% sodium dodecyl sulfate-polyacrylamide gel electrophoresis (SDS-PAGE) and then transferred onto polyvinylidene fluoride membranes (PVDF; Millipore, Billerica, MA, USA). The membranes were blocked with 5% non-fat milk in Tris buffered saline and 0.1% Tween-20 (TBST) at room temperature to reduce nonspecific bindings of antibodies. The blots were probed with primary antibodies overnight at 4 °C to ALP (Huabio, Hangzhou, China), RUNX2 (Proteintech, Hubei, China), OPG (Abcam, Cambridge, UK), RANKL and GAPDH (Proteintech, Hubei, China). After washing in TBST, the membrane was incubated with the corresponding secondary antibody (Absin, Shanghai, China) at 37 °C for 1 hour. We used an enhanced chemiluminescent substrate kit (Biosharp, Anhui, China) to visualize the immunoreactive proteins. ImageJ software (NIH, Bethesda, MD, USA) was used to quantitatively analyze the protein expression.

## Statistical Analysis

All experiments were conducted at least three times. The results were analyzed by GraphPad Prism 8 (GraphPad Software, Inc., La Jolla, CA, USA) and expressed as mean  $\pm$  standard deviation (mean  $\pm$  SD). Shapiro–Wilk test was used to evaluate normality, and the differences between each group were analyzed by Student's unpaired *t*-test and one-way analysis of variance (ANOVA). *P*-value  $< 0.05$  was considered statistically significant.

## Results

### Animal Experiment

#### Animal Condition

All rats survived well in the experiment. Their weight showed an upward trend within 14 days, and there were no difference in weight among different groups. There were no other adverse events during study period.

#### Orthodontic Tooth Movement Measurements

The OTM of high-dose group (40 mg/kg) and low-dose group (20 mg/kg) were  $0.35\text{mm} \pm 0.04\text{mm}$  and  $0.40\text{mm} \pm 0.03\text{mm}$ , respectively, which was significantly lower than control group ( $0.47\text{mm} \pm 0.04\text{mm}$ ). There was a statistical difference between sinomenine groups and the control group, and the decrease of OTM in high-dose group was more obvious (Figure 2A).

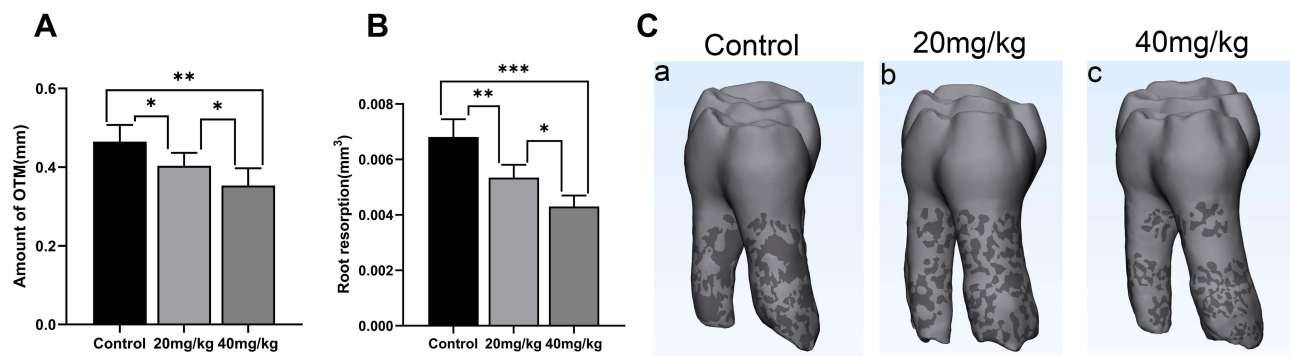


**Figure 2** Amount of tooth movement and root resorption. (A) After 14 days of orthodontic treatment, the OTM was inhibited by sinomenine. (B) The root resorption volume of sinomenine-treated groups was significantly lower than control group. (C) Micro-CT reconstructed image showed the root resorption area of the all groups. Distal view of the right maxillary first molar of control group (a), 20 mg/kg sinomenine group (b) and 40 mg/kg sinomenine group (c). Dark areas show the resorption areas. Data are expressed as mean  $\pm$  SD (\* $P < 0.05$ , \*\* $P < 0.01$ , \*\*\* $P < 0.001$ ).

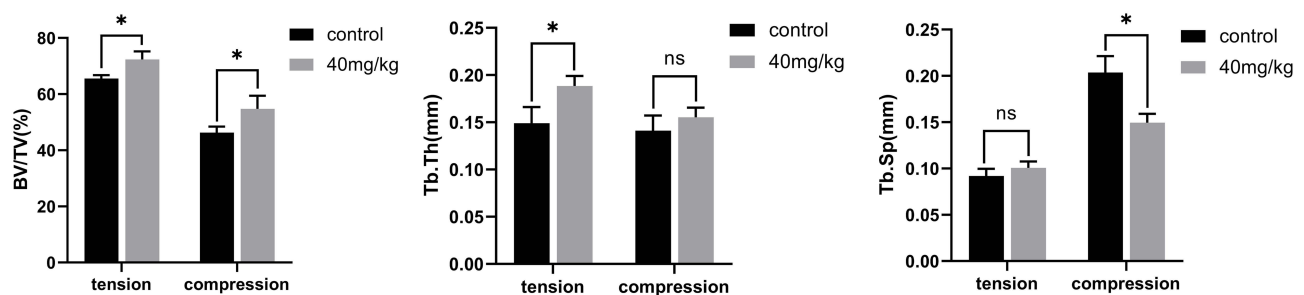


**Figure 3** Evaluation of trabecular bone on day 14. Bone volume/total volume (BV/TV), trabecular thickness (Tb.Th) and trabecular separation (Tb.Sp) of control group and 40 mg/kg sinomenine group at the compression side and tension side. Data are expressed as mean  $\pm$  SD (\* $P < 0.05$ ).

## The Volume of Root Resorption

The root resorption area can be observed in all groups, and the resorption volume of sinomenine groups was significantly lower than that of the control group (Figure 2B and C). Compared with the low-dose group (20 mg/kg), the high-dose group (40 mg/kg) had the least root resorption.

## Evaluation of Trabecular Bone

The evaluation of alveolar bone on day 14 is shown in Figure 3. On the tension side, BV/TV and Tb.Th of 40 mg/kg sinomenine group increased significantly ( $P < 0.05$ ), but there was no significant difference in Tb.Sp. On the compression side, compared with the control group, bone volume/total volume (BV/TV) of 40 mg/kg sinomenine group increased significantly ( $P < 0.05$ ). Trabecular thickness (Tb.Th) increased slightly, but there was no significant difference. Trabecular separation (Tb.Sp) decreased significantly ( $P < 0.05$ ).

## Masson Staining Observation

On the compression side, the periodontal ligament was squeezed, the fibers were arranged disorderly, and resorption lacunae could be observed on the surface of alveolar bone and root. The resorption lacunae in control group was the largest, and the resorption area in the sinomenine group decreased in a concentration-dependent manner. Red blood cell extravasation was observed in the periodontal ligament space. On the tension side, the periodontal ligament width was enlarged and the fiber bundle was pulled and elongated. The collagen fibers in sinomenine groups were arranged regularly and tightly. Active osteoblasts forming new bone could be observed near alveolar bone, especially in high concentration sinomenine group (Figure 4).

## TRAP Staining Observation

After 14 days of treatment, red-stained cells were observed on the compression side of the root of the maxillary first molar, which were TRAP-positive cells (Figure 5). In the control group, a large amount of TRAP-positive osteoclasts and odontoclasts were observed on the alveolar bone and root surface. The number of TRAP-positive multinuclear cells around the compression side in sinomenine-treated groups decreased significantly. TRAP-positive cells in 40 mg/kg group were significantly less than those in 20 mg/kg group. In addition, TRAP-positive cells of sinomenine groups were mainly located on the alveolar bone.

## Immunohistological Staining Analysis

Immunohistochemical (IHC) staining was performed to observe the expression of TNF- $\alpha$ , RANKL and OPG on the compression side of periodontal area (Figure 6A–C) and the immunoreactivity of RUNX2 and OCN on the tension side of periodontium (Figure 6D and E). Compared with the control group, the expressions of RANKL and TNF- $\alpha$  in sinomenine-treated groups decreased significantly. Conversely, the expressions of OPG, RUNX2 and OCN in sinomenine-treated groups were significantly higher than those in control group ( $p < 0.01$ ).

## Cell Experiment

### Cultivation and Characterization of PDLSCs

PDLSCs were successfully cultivated from periodontal ligament tissue (Figure 7A). After 21 days of adipogenic and osteogenic induction, oil red O staining (Figure 7B) and alizarin red staining (Figure 7C) showed the accumulation of lipid droplets and the formation of mineralized nodules, indicating that PDLSCs have the potential of lipogenic and osteogenic differentiation. The expression level of surface markers of PDLSCs was detected by flow cytometry. The results showed that the expression of mesenchymal stem cell (MSC) specific surface markers CD90 and CD105 were positive (Figure 7G and H), while the hematopoietic stem cells (HSCs) marker CD34 (Figure 7E) and pan-leukocyte marker CD45 were absent (Figure 7F).

### Cell Proliferation Assay

On days 0, 1, 3 and 5, the effects of various concentrations of sinomenine (0M, 0.1 M, 0.2 M, 0.5 M, 1.0 M and 2.0 M) on the proliferation of PDLSCs were determined by CCK-8 assays (Figure 8A). On day 1, there were no significant differences among all groups. On day 3, 1.0 M and 2.0 M sinomenine inhibited the proliferation of PDLSCs ( $P < 0.05$ ). On day 5, compared with the control group, 0.1 M sinomenine promoted the proliferation of cells ( $P < 0.01$ ), 0.2 M and



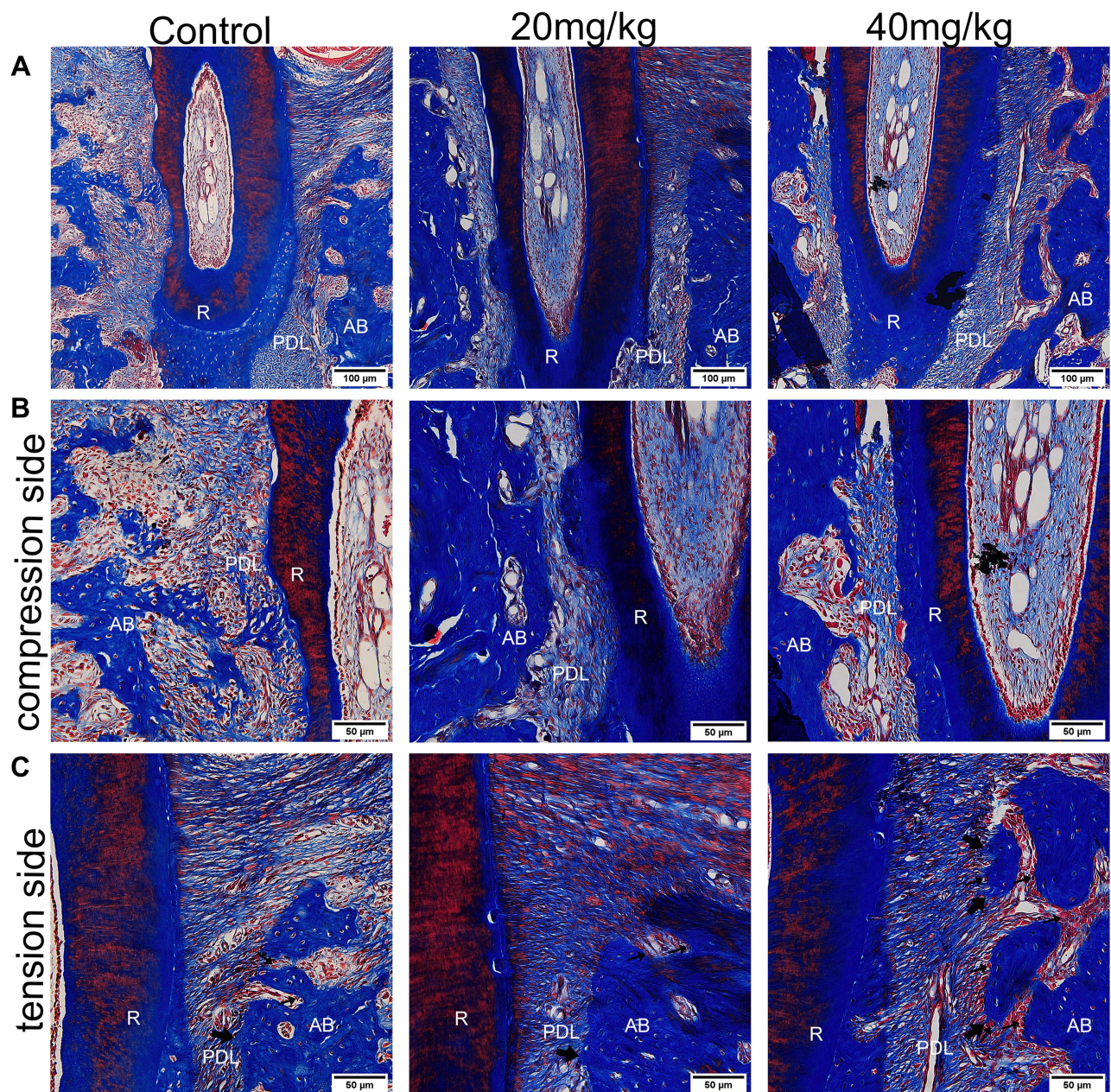


**Figure 4** Results of Masson's trichrome staining. **(A)** The periodontal ligament on the compression side was squeezed and the width of periodontal ligament on the tension side enlarged. Scale Bar: 100  $\mu\text{m}$ . **(B)** Enlarged view of the compression side. Resorption lacunae could be observed on the surface of alveolar bone and root. Scale Bar: 50  $\mu\text{m}$ . **(C)** Enlarged view of the tension side. The fiber bundle is pulled and elongated. The collagen fibers in sinomenine groups were arranged regularly and tightly. Active osteoblasts forming new bone were most obvious in 40 mg/kg sinomenine group. The small arrows indicate the osteoblast. The large arrows indicate the new bone. Scale Bar: 50  $\mu\text{m}$ . **Abbreviations:** AB, alveolar bone; PDL, periodontal ligament; R, root.

0.5 M sinomenine had no significant effect on cell proliferation, while high concentration of sinomenine (1.0 M and 2.0 M) significantly inhibited the proliferation of PDLSCs (Figure 8B).

#### Sinomenine Enhanced Mineralized Nodule Deposition and ALP Activity

Alizarin red staining was used to observe mineral deposition (Figure 8C). The results indicated that 0.1 M and 0.5 M sinomenine markedly promoted the deposition of mineralized nodules compared with the control group (Figure 8D) and showed a dose-dependent increasing trend. In the ALP activity assays (Figure 8E), it was found that on day 7, the ALP activity in 0.1 M and 0.5 M sinomenine groups increased significantly.



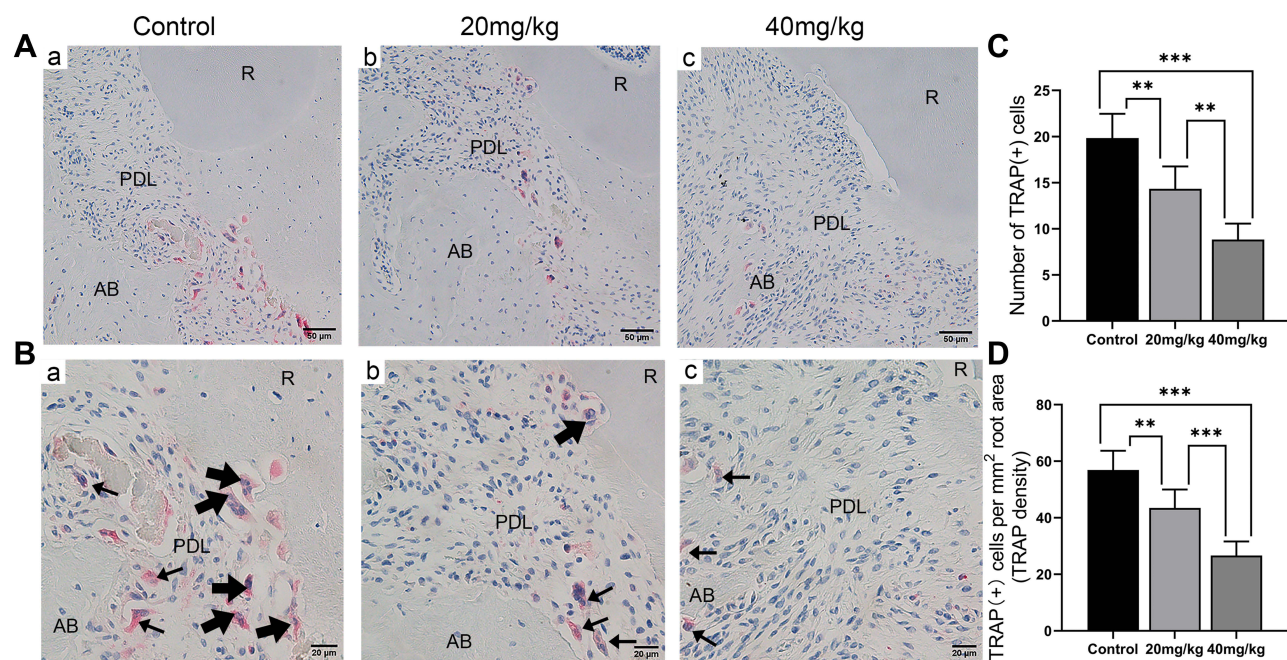


**Figure 5** TRAP staining of maxillary first molar after 14 days of OTM. **(A)** The TRAP staining of the control group (a), 20 mg/kg group (b) and 40 mg/kg group (c). Scale Bar: 50  $\mu$ m. **(B)** Enlarged view of **(A)**. The number of TRAP-positive multinuclear cells in sinomenine groups were significantly lower than control group. The small arrows indicate the osteoclasts. The large arrows indicate the odontoclasts. Scale Bar: 20  $\mu$ m. **(C)** Number of TRAP-positive cells in the mesial side of the distopalatal root. **(D)** Quantitative analysis of TRAP-positive cells was further performed by calculating the number of TRAP-positive cells on the mesial side of the distopalatal root/the distopalatal root area within the same slice. Data are expressed as mean  $\pm$  SD (\*\* $P$ <0.01, \*\*\* $P$ <0.001).

**Abbreviations:** AB, alveolar bone; PDL, periodontal ligament; R, root.

## Osteogenesis-Associated mRNA and Protein Expression

After 7 days of osteogenic induction, the expression levels of osteogenesis-related factors ALP and RUNX2 were analyzed (Figure 8F–G). Compared with the control group, the mRNA expressions of ALP and RUNX2 in sinomenine-treated groups were up-regulated in a concentration-dependent manner. Western blot indicated that the expression of osteogenesis-related protein ALP and RUNX2 showed a dose-dependent upward trend.

## Sinomenine Regulates OPG/RANKL Pathway

The expression levels of OPG/RANKL pathway-related factors RANKL and OPG were analyzed on day 7. In sinomenine groups, the mRNA and protein expressions of RANKL (Figure 9A and D) decreased compared with the control group, while the mRNA and protein expressions of OPG (Figure 9B and E) were up-regulated. Compared with the control group, RANKL/OPG of sinomenine groups showed a decreasing trend (Figure 9C and F).

## Discussion

In this research, we investigated the effect of sinomenine on tooth movement and root resorption during OTM by establishing an animal model, the effect of sinomenine on osteogenic differentiation of PDLSCs in vitro, and the potential mechanism of sinomenine on bone metabolism. The dynamic balance of bone resorption and bone formation plays a key role in bone remodeling. OTM is the result of different relative activities of bone resorption and formation on the compression side and tension side under mechanical stimulation. Tooth load leads to local hypoxia and fluid flow, which leads to aseptic inflammatory cascade, and finally leads active osteoclasts on the compression side to produce bone resorption and osteoblasts in the tension area to produce bone deposition.<sup>43</sup> In this process, inflammatory mediators, such as prostaglandin E2 (PGE2), interleukin 1 (IL-1), interleukin 6 (IL-6), transforming growth factor beta (TGF- $\beta$ ), and tumor necrosis factor- $\alpha$  (TNF- $\alpha$ ), are involved in the activation of osteoclasts, which eventually leads to the loss of bone on the compression side and the movement of tooth. Previous studies have shown that many endogenous and exogenous substances could affect OTM and root resorption. Strontium ranelate can improve tooth anchorage and reduce root



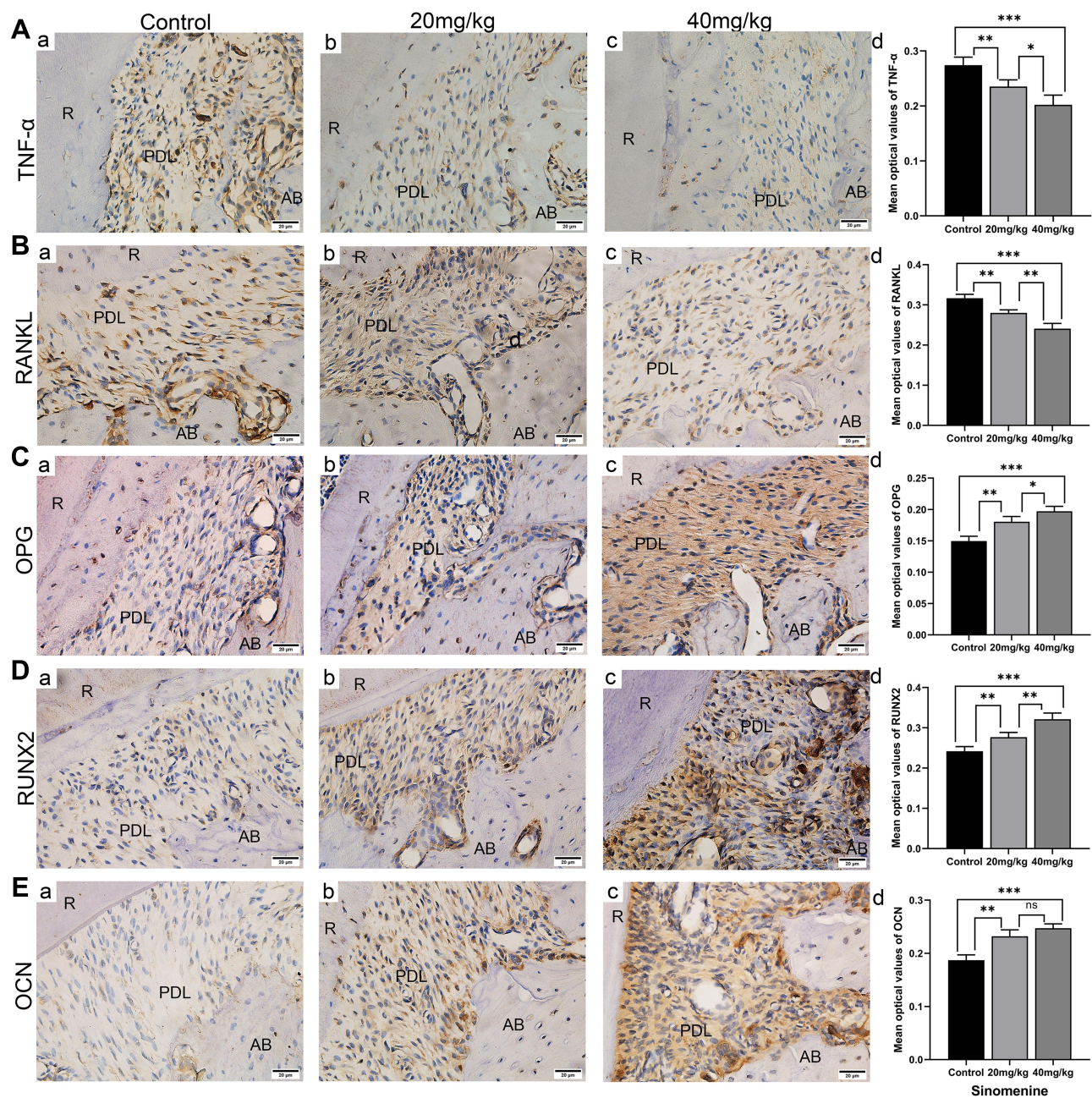


**Figure 6** Results of immunohistochemical staining. (A–B) The result of TNF- $\alpha$  (A) and RANKL (B) immunostaining of the maxillary first molar indicated that the expression of TNF- $\alpha$  and RANKL decreased in sinomenine-treated groups. (C–E) The results of OPG (C), RUNX2 (D) and OCN (E) IHC staining indicated that the expression of OPG, RUNX2 and OCN increased. Scale Bar: 20  $\mu$ m. Data are expressed as mean  $\pm$  SD (\*  $P < 0.05$ , \*\* $P < 0.01$ , \*\*\* $P < 0.001$ ).

**Abbreviations:** AB, alveolar bone; PDL, periodontal ligament; R, root.

resorption in rat OTM model.<sup>44</sup> Aspirin can inhibit tooth movement and orthodontic recurrence.<sup>45,46</sup> Resveratrol can significantly reduce the degree of OTM distance and the proportion of OIRR in rat model.<sup>47</sup> Nicotine can increase tooth movement speed and OIRR.<sup>48</sup>

Sinomenine can regulate bone metabolism. Previous studies have shown that sinomenine could inhibit the osteoclastic differentiation of mesenchymal stem cells<sup>36</sup> and promote osteogenic differentiation of MC3T3-E1 cells by regulating Akt/Runx2 signaling pathway.<sup>34</sup> In addition, many studies have shown that sinomenine has anti-inflammatory effects,<sup>26–28</sup> which has been used in the treatment of systemic lupus erythematosus and rheumatoid arthritis for many years. It has been found that sinomenine can downregulate inflammatory cytokines (TNF- $\alpha$ , IL-1 and IL-6), which significantly inhibited the



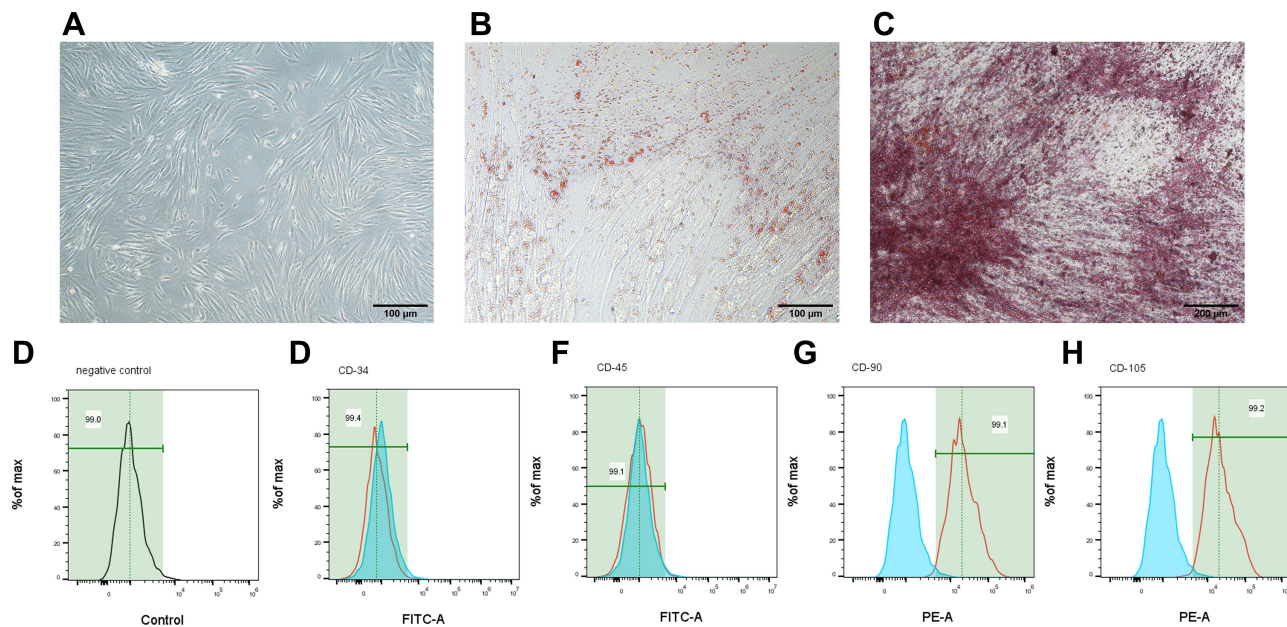


**Figure 7** Cultivation and characterization of PDLSCs. **(A)** PDLSCs showed a long spindle-shaped form. Scale Bar: 100  $\mu$ m. **(B)** After adipogenic induction, PDLSCs were stained with oil red O. Scale bar: 100  $\mu$ m. **(C)** After osteogenic induction, PDLSCs were stained with alizarin red. Scale bar: 200  $\mu$ m. **(D–H)** Surface markers observed under flow cytometry. The expression of CD34 **(E)** and CD45 **(F)** were negative, while CD90 **(G)** and CD105 **(H)** were positive. Figure D and color blue represented negative control.

immune response of macrophages stimulated by LPS.<sup>49</sup> In view of the effect of sinomenine on bone metabolism and its wide clinical application, exploring the effect of sinomenine on OTM may provide some value for the clinical treatment of orthodontic patients taking sinomenine.

In the present study, it was observed that the number of TRAP-positive cells on the surface of alveolar bone and roots of rats treated with sinomenine decreased. Micro-CT analysis showed that BV/TV on the compression side of sinomenine groups increased, while Tb.Sp decreased. These results indicate that sinomenine may inhibit the activation of osteoclasts and increase trabecular bone mass. Considering the significant anti-inflammatory effect of sinomenine, and inflammation will activate osteoclasts, the reduction of bone resorption in the sinomenine groups may also be related to the anti-inflammatory characteristics of sinomenine, which may be similar to the principle of some anti-inflammatory drugs such as aspirin to inhibit tooth movement.<sup>50</sup> The results of immunohistochemistry showed that sinomenine reduced the expression of TNF- $\alpha$ , which confirmed that sinomenine reduced the inflammatory cytokines during tooth movement. TNF- $\alpha$  plays an important role during OTM. The number of TRAP-positive osteoclasts and the rate of tooth movement in mice with TNF receptor deficiency were significantly decreased.<sup>51,52</sup> In addition, previous evidence supports that TNF- $\alpha$  and RANKL have a synergistic effect on osteoclast differentiation, and TNF- $\alpha$  can enhance the osteoclastogenic response to RANKL.<sup>53</sup> The inhibition of sinomenine on TRAP-positive osteoclasts and tooth movement may be closely related to the reduction of TNF- $\alpha$  and other inflammatory cytokines. Inflammation can also cause root resorption as a side effect during OTM.<sup>54</sup> The mechanism of OIRR is similar to that of osteoclasts induced bone resorption. The inhibition of sinomenine on the activation of osteoclasts may also be the reason for the decrease of OIRR.

The increase of BV/TV and Tb.Th of 40 mg/kg sinomenine group on the tension side indicates that sinomenine may promote bone formation. Immunohistochemical staining of RUNX2 and OCN also confirmed that sinomenine may promote osteogenesis. Therefore, this study further explored the effect of sinomenine on osteogenesis through the in vitro experiment. We chose PDLSCs as the research cells, because PDLSCs play an important role in the remodeling of periodontal ligament and alveolar bone during OTM.<sup>19</sup> In addition, the multidirectional differentiation potential, strong self-renewal ability, and high periodontal correlation of PDLSCs also make PDLSCs reliable seed cells in periodontal tissue regeneration engineering. If sinomenine can promote bone formation, sinomenine may play a role in the field of tissue regeneration and have a certain significance for periodontal tissue regeneration engineering.



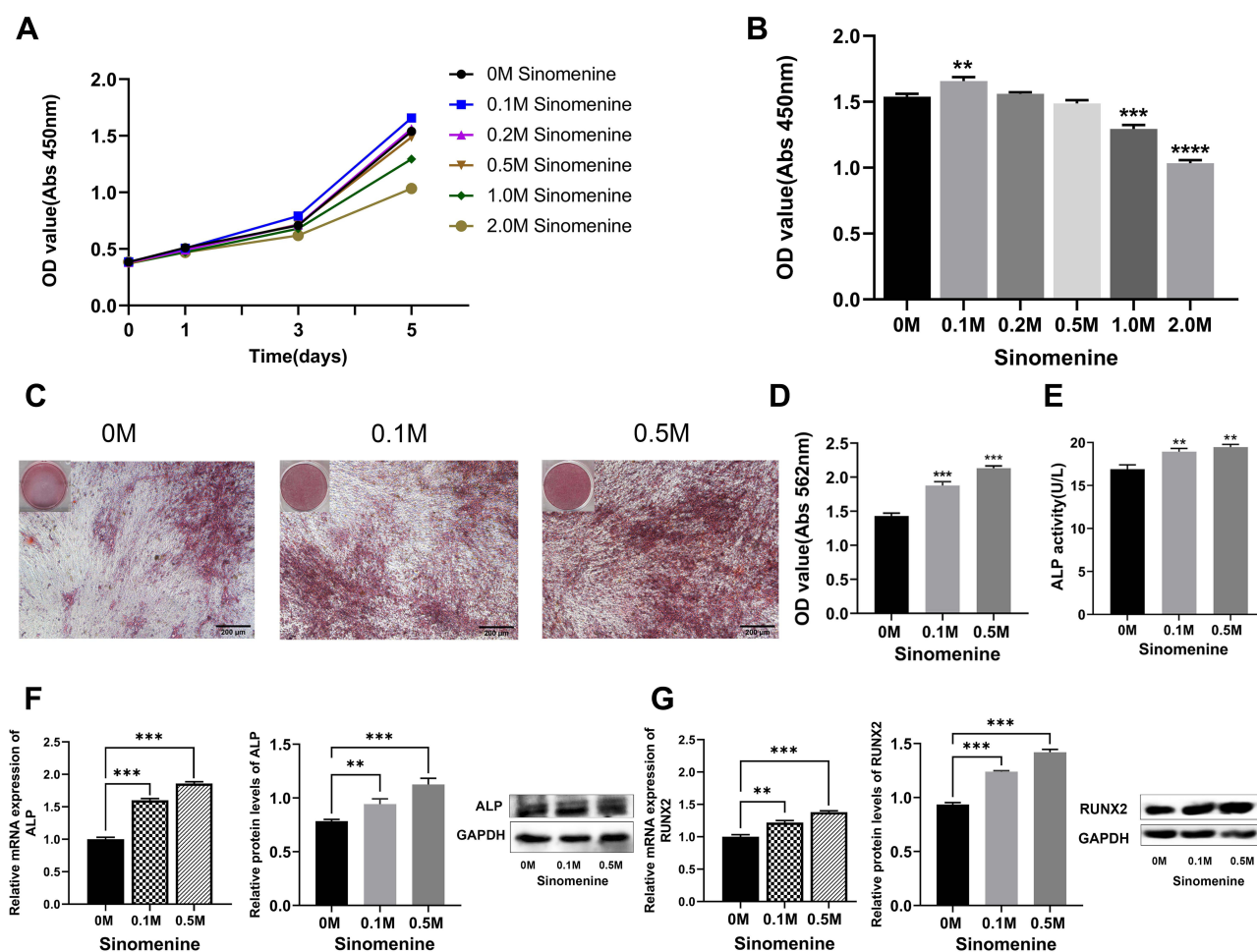


**Figure 8** Effect of sinomenine on proliferation and osteogenesis of PDLSCs. **(A)** PDLSCs were treated with 0, 0.1 M, 0.2 M, 0.5 M, 1.0 M, 2.0 M sinomenine for 0, 1, 3, and 5 days, and the growth curves were depicted according to the results of CCK-8 assay. **(B)** 0.1 M sinomenine stimulated the proliferation of PDLSCs, while 1.0 M and 2.0 M sinomenine markedly inhibited the proliferation of PDLSCs on day 5. **(C)** Mineral deposition was observed by Alizarin red staining. Scale bar: 200  $\mu$ m. **(D)** The relative amount of mineralized nodule was assessed based on the absorbance at 562 nm. **(E)** ALP activity was enhanced by 0.1 M and 0.5 M sinomenine at day 7. **(F and G)** The mRNA and protein expression levels of ALP **(F)** and RUNX2 **(G)** in sinomenine-treated groups for 7 days. Data are presented as mean  $\pm$  SD (\*\* $P$ <0.01, \*\*\* $P$ <0.001, \*\*\*\* $P$ <0.0001).

In our study, PDLSCs were isolated and obtained by tissue block method. The cells were identified by flow cytometry analysis and multidirectional differentiation culture. Through CCK-8 assays, it was determined that low concentration of sinomenine (0.1 M, 0.2 M and 0.5 M) did not inhibit cell proliferation, which is similar to the study previously.<sup>36</sup> It was determined by ALP activity and alizarin red staining that sinomenine at concentrations of 0.1 M and 0.5 M promoted the osteogenesis of PDLSCs, which was consistent with the previously reported result that sinomenine promoted the differentiation of osteoblasts.<sup>34</sup> This study further evaluated the effect of sinomenine on the osteogenic differentiation of PDLSCs by analyzing the expression of osteogenic related mRNA and proteins. ALP and RUNX2 were selected as indicators of osteogenesis-associated factors. ALP is an early detection index of osteogenesis. The increase of ALP activity reflects the beginning of osteoblast calcification.<sup>55</sup> RUNX2 is regarded as a critical transcription factor for osteogenesis and is related to the activation of bone-specific genes.<sup>56</sup> The results of qRT-PCR and Western blot showed that sinomenine significantly increased the expression levels of osteogenesis-associated mRNA and protein.

We further studied the expression of mRNA and protein related to RANKL/OPG pathway. The results indicated that sinomenine promoted the mRNA transcription and protein expression of OPG and inhibited the expression of RANKL, which was consistent with the results of immunohistochemical staining in rats. This suggests that the mechanism of sinomenine inhibiting OTM and OIRR may be through RANKL/OPG pathway. RANKL, a key factor in the formation

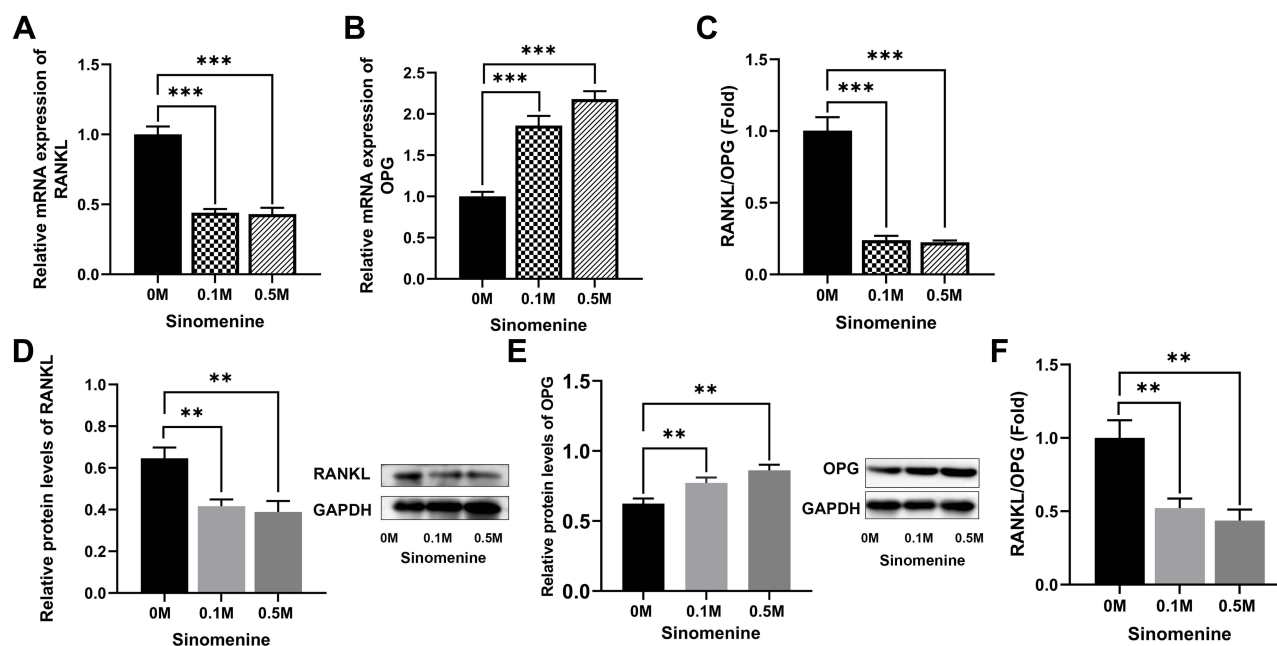


**Figure 9** Effect of sinomenine on OPG/RANKL pathway. The mRNA and protein expression levels of RANKL (**A** and **D**) and OPG (**B** and **E**) in sinomenine-treated groups and control group at day 7. RANKL/OPG expression is inhibited by sinomenine on both mRNA (**C**) and protein (**F**) level. Data are expressed as mean  $\pm$  SD (\*\* $P$ <0.01, \*\*\* $P$ <0.001).

and activation of osteoclasts and odontoclasts, mainly expressed by osteocytes, osteoblasts and stromal cells, plays a significant role in promoting osteoclast differentiation by binding to RANK on the surface of osteoclast precursor cells. As a decoy receptor, OPG competes with RANK for binding to RANKL, resulting in the inhibition of osteoclast activation and differentiation and the occurrence of osteoclast apoptosis. In the environment with appropriate concentration of sinomenine, PDLSCs could express more OPG and less RANKL, which may further inhibit the activity of osteoclasts and inhibit tooth movement and root resorption in rats.

Based on the above, we confirmed the hypothesis that sinomenine inhibits OTM and root resorption in rats and promotes osteogenic differentiation of PDLSCs. We infer that sinomenine may prevent bone resorption, promote bone formation, improve tooth anchorage and reduce OIRR. The mechanism of sinomenine inhibiting OTM and root resorption in rats may be related to RANKL/OPG pathway.

It should be noted that the results of animal studies research do not always be extended to humans, because the bone structure, physiological response, drug dose, force size, force duration between human and rats are different. Moreover, the in-depth mechanism is not completely clear. In addition, the limitation of this study was that only the short-term effect of sinomenine on orthodontic treatment in rats has been studied *in vivo*, while orthodontic treatment is a long-term process, and the long-term effect needs to be further evaluated.

## Conclusion

In the present study, we demonstrated that sinomenine inhibited the movement and root resorption of orthodontic tooth. Sinomenine improved the structure of alveolar bone in rats and induced a significant increase in BV/TV. Sinomenine significantly reduced TRAP-positive osteoclasts and suppressed the expression of the inflammatory cytokines TNF- $\alpha$  on the compression side. Sinomenine significantly decreased the expression of RANKL/OPG on the compression side, in which the expression of RANKL was significantly decreased and the expression of OPG was increased. In addition, sinomenine enhanced the expression of OCN and RUNX2 on the tension side. We further found that sinomenine could promote the expression of ALP and RUNX2 in PDLSCs and improve the deposition of mineralized nodules. In conclusion, our results show that sinomenine could inhibit orthodontic tooth movement and root resorption in rats by

inhibiting the activity of osteoclasts through RANKL/OPG pathway. In addition, sinomenine had a positive effect on bone formation at the tension side and promoted the osteogenic differentiation of PDLSCs.

## Abbreviations

PDLSCs, periodontal ligament stem cells; Micro-CT, Micro-computed tomography; TRAP, tartrate-resistant acid phosphatase; ALP, Alkaline phosphatase; RUNX2, runt-related transcription factor 2; RANKL, receptor activator of nuclear factor kappaB ligand; OPG, osteoprotegerin; OCN, osteocalcin; OTM, orthodontic tooth movement; ARO, autosomal recessive osteopetrosis; OIRR, orthodontic induced root resorption; SIN, sinomenine; EDTA, ethylenediaminetetraacetic acid; ROI, regions of interest; BV/TV, bone volume/total volume; Tb.Th, trabecular thickness; Tb.Sp, trabecular separation/spacing; HRP, horseradish peroxidase; PBS, phosphate buffered saline; FBS, fetal bovine serum;  $\alpha$ -MEM,  $\alpha$ -minimum essential medium; CCK-8, Cell Counting Kit-8; BCA, bicinchoninic acid assay; CPC, cetylpyridinium chloride; qRT-PCR, quantitative real-time; GAPDH, glyceraldehyde-3-phosphate dehydrogenase; SDS-PAGE, sodium dodecyl sulfate-polyacrylamide gel electrophoresis; PVDF, polyvinylidene fluoride membranes.

## Acknowledgments

This work was supported by the Natural Science Foundation of Shandong Province (ZR2021QH340) and the Horizontal Scientific Research Fund of Shandong University (1350022003).

## Disclosure

The authors report no conflicts of interest in this work.

## References

1. Meikle MC. The tissue, cellular, and molecular regulation of orthodontic tooth movement: 100 years after Carl Sandstedt. *Eur J Orthod.* 2006;28(3):221–240. doi:10.1093/ejo/cjl001
2. Yasuda H, Shima N, Nakagawa N, et al. Osteoclast differentiation factor is a ligand for osteoprotegerin/osteoclastogenesis-inhibitory factor and is identical to TRANCE/RANKL. *Proc Natl Acad Sci USA.* 1998;95(7):3597–3602. doi:10.1073/pnas.95.7.3597
3. Udagawa N, Koide M, Nakamura M, et al. Osteoclast differentiation by RANKL and OPG signaling pathways. *J Bone Miner Metab.* 2021;39(1):19–26. doi:10.1007/s00774-020-01162-6
4. Kobayashi Y, Udagawa N, Takahashi N. Action of RANKL and OPG for osteoclastogenesis. *Crit Rev Eukaryot Gene Expr.* 2009;19(1):61–72. doi:10.1615/critrevukargeneexpr.v19.i1.30
5. Yasuda H, Shima N, Nakagawa N, et al. Identity of osteoclastogenesis inhibitory factor (OCIF) and osteoprotegerin (OPG): a mechanism by which OPG/OCIF inhibits osteoclastogenesis in vitro. *Endocrinology.* 1998;139(3):1329–1337. doi:10.1210/endo.139.3.5837
6. Iglesias-Linares A, Moreno-Fernandez AM, Yañez-Vico R, Mendoza-Mendoza A, Gonzalez-Moles M, Solano-Reina E. The use of gene therapy vs. corticotomy surgery in accelerating orthodontic tooth movement. *Orthod Craniofac Res.* 2011;14(3):138–148. doi:10.1111/j.1601-6343.2011.01519.x
7. Kanzaki H, Chiba M, Takahashi I, Haruyama N, Nishimura M, Mitani H. Local OPG gene transfer to periodontal tissue inhibits orthodontic tooth movement. *J Dent Res.* 2004;83(12):920–925. doi:10.1177/154405910408301206
8. Sobacchi C, Frattini A, Guerrini MM, et al. Osteoclast-poor human osteopetrosis due to mutations in the gene encoding RANKL. *Nat Genet.* 2007;39(8):960–962. doi:10.1038/ng2076
9. Lo Iacono N, Pangrazio A, Abinun M, et al. RANKL cytokine: from pioneer of the osteoimmunology era to cure for a rare disease. *Clin Dev Immunol.* 2013;2013:412768. doi:10.1155/2013/412768
10. Lo Iacono N, Blair HC, Poliani PL, et al. Osteopetrosis rescue upon RANKL administration to Rankl(-/-) mice: a new therapy for human RANKL-dependent ARO. *J Bone Miner Res.* 2012;27(12):2501–2510. doi:10.1002/jbmr.1712
11. Kong YY, Yoshida H, Sarosi I, et al. OPGL is a key regulator of osteoclastogenesis, lymphocyte development and lymph-node organogenesis. *Nature.* 1999;397(6717):315–323. doi:10.1038/16852
12. Seo BM, Miura M, Gronthos S, et al. Investigation of multipotent postnatal stem cells from human periodontal ligament. *Lancet.* 2004;364(9429):149–155. doi:10.1016/S0140-6736(04)16627-0
13. Kadar K, Kiraly M, Porcsalmy B, et al. Differentiation potential of stem cells from human dental origin - promise for tissue engineering. *J Physiol Pharmacol.* 2009;60(Suppl 7):167–175.
14. Mrozik K, Gronthos S, Shi S, Bartold PM. A method to isolate, purify, and characterize human periodontal ligament stem cells. *Methods Mol Biol.* 2017;1537:413–427. doi:10.1007/978-1-4939-6685-1\_24
15. Mrozik KM, Wada N, Marino V, et al. Regeneration of periodontal tissues using allogeneic periodontal ligament stem cells in an ovine model. *Regen Med.* 2013;8(6):711–723. doi:10.2217/rme.13.66
16. Liu Y, Zheng Y, Ding G, et al. Periodontal ligament stem cell-mediated treatment for periodontitis in miniature swine. *Stem Cells.* 2008;26(4):1065–1073. doi:10.1634/stemcells.2007-0734
17. Park SY, Kim KH, Gwak EH, et al. Ex vivo bone morphogenetic protein 2 gene delivery using periodontal ligament stem cells for enhanced re-osseointegration in the regenerative treatment of peri-implantitis. *J Biomed Mater Res A.* 2015;103(1):38–47. doi:10.1002/jbm.a.35145

18. Kato T, Hattori K, Deguchi T, et al. Osteogenic potential of rat stromal cells derived from periodontal ligament. *J Tissue Eng Regen Med.* 2011;5(10):798–805. doi:10.1002/term.379
19. Huang H, Yang R, Zhou YH. Mechanobiology of periodontal ligament stem cells in orthodontic tooth movement. *Stem Cells Int.* 2018;2018:6531216. doi:10.1155/2018/6531216
20. Zhang L, Liu W, Zhao J, et al. Mechanical stress regulates osteogenic differentiation and RANKL/OPG ratio in periodontal ligament stem cells by the Wnt/ $\beta$ -catenin pathway. *Biochim Biophys Acta.* 2016;1860(10):2211–2219. doi:10.1016/j.bbagen.2016.05.003
21. Feng L, Yang R, Liu D, et al. PDL progenitor-mediated PDL recovery contributes to orthodontic relapse. *J Dent Res.* 2016;95(9):1049–1056. doi:10.1177/0022034516648604
22. Liu J, Li Q, Liu S, et al. Periodontal ligament stem cells in the periodontitis microenvironment are sensitive to static mechanical strain. *Stem Cells Int.* 2017;2017:1380851. doi:10.1155/2017/1380851
23. Zhang C, Lu Y, Zhang L, et al. Influence of different intensities of vibration on proliferation and differentiation of human periodontal ligament stem cells. *Arch Med Sci.* 2015;11(3):638–646. doi:10.5114/aoms.2015.52370
24. Gao Q, Walmsley AD, Cooper PR, Scheven BA. Ultrasound stimulation of different dental stem cell populations: role of mitogen-activated protein kinase signaling. *J Endod.* 2016;42(3):425–431. doi:10.1016/j.joen.2015.12.019
25. Li B, Zhang Y, Wang Q, et al. Periodontal ligament stem cells modulate root resorption of human primary teeth via Runx2 regulating RANKL/OPG system. *Stem Cells Dev.* 2014;23(20):2524–2534. doi:10.1089/scd.2014.0127
26. Zhou H, Liu JX, Luo JF, et al. Suppressing mPGES-1 expression by sinomenine ameliorates inflammation and arthritis. *Biochem Pharmacol.* 2017;142:133–144. doi:10.1016/j.bcp.2017.07.010
27. Liu W, Zhang Y, Zhu W, et al. Sinomenine inhibits the progression of rheumatoid arthritis by regulating the secretion of inflammatory cytokines and monocyte/macrophage subsets. *Front Immunol.* 2018;9:2228. doi:10.3389/fimmu.2018.02228
28. Wang Q, Li XK. Immunosuppressive and anti-inflammatory activities of sinomenine. *Int Immunopharmacol.* 2011;11(3):373–376. doi:10.1016/j.intimp.2010.11.018
29. Kiasalari Z, Afshin-Majd S, Baluchnejadmojarad T, et al. Sinomenine alleviates murine experimental autoimmune encephalomyelitis model of multiple sclerosis through inhibiting NLRP3 inflammasome. *J Mol Neurosci.* 2021;71(2):215–224. doi:10.1007/s12031-020-01637-1
30. Qin T, Yin S, Yang J, et al. Sinomenine attenuates renal fibrosis through Nrf2-mediated inhibition of oxidative stress and TGF $\beta$  signaling. *Toxicol Appl Pharmacol.* 2016;304:1–8. doi:10.1016/j.taap.2016.05.009
31. Geng P, Xu X, Gao Z. Sinomenine suppress the vitamin D3 and high fat induced atherosclerosis in rats via suppress of oxidative stress and inflammation [published correction appears in *J Oleo Sci.* 2022;71(4):628]. *J Oleo Sci.* 2021;70(12):1815–1828. doi:10.5650/jos.ess21255
32. Zhang MW, Wang XH, Shi J, Yu JG. Sinomenine in cardio-cerebrovascular diseases: potential therapeutic effects and pharmacological evidences. *Front Cardiovasc Med.* 2021;8:749113. doi:10.3389/fcvm.2021.749113
33. Li XM, Li MT, Jiang N, et al. Network pharmacology-based approach to investigate the molecular targets of sinomenine for treating breast cancer. *Cancer Manag Res.* 2021;13:1189–1204. doi:10.2147/CMAR.S282684
34. Zhang B, Zhang H, Luo H, Yang C, Yuan Y. Sinomenine can promote the proliferation and differentiation of osteoblasts by regulating the Akt/Runx2 signaling pathway in MC3T3-E1 cells. *Pharmazie.* 2019;74(12):747–750. doi:10.1691/ph.2019.9636
35. Liao K, Su X, Lei K, et al. Sinomenine protects bone from destruction to ameliorate arthritis via activating p62Thr269/Ser272-Keap1-Nrf2 feedback loop. *Biomed Pharmacother.* 2021;135:111195. doi:10.1016/j.biopha.2020.111195
36. Zhou B, Lu X, Tang Z, et al. Influence of sinomenine upon mesenchymal stem cells in osteoclastogenesis. *Biomed Pharmacother.* 2017;90:835–841. doi:10.1016/j.biopha.2017.03.084
37. du Sert N P, Hurst V, Ahluwalia A, et al. The ARRIVE guidelines 2.0: updated guidelines for reporting animal research. *PLoS Biol.* 2020;18(7):e3000410. doi:10.1371/journal.pbio.3000410
38. Ullrich N, Schröder A, Bauer M, et al. The role of HIF-1 $\alpha$  in nicotine-induced root and bone resorption during orthodontic tooth movement. *Eur J Orthod.* 2021;43(5):516–526. doi:10.1093/ejo/cjaa057
39. Ino-Kondo A, Hotokezaka H, Kondo T, et al. Lithium chloride reduces orthodontically induced root resorption and affects tooth root movement in rats. *Angle Orthod.* 2018;88(4):474–482. doi:10.2319/112017-801.1
40. Yang F, Wang XX, Ma D, et al. Effects of triptolide on tooth movement and root resorption in rats. *Drug Des Devel Ther.* 2019;13:3963–3975. doi:10.2147/DDDT.S217936
41. Nie F, Zhang W, Cui Q, Fu Y, Li H, Zhang J. Kaempferol promotes proliferation and osteogenic differentiation of periodontal ligament stem cells via Wnt/ $\beta$ -catenin signaling pathway. *Life Sci.* 2020;258:118143. doi:10.1016/j.lfs.2020.118143
42. Livak KJ, Schmittgen TD. Analysis of relative gene expression data using real-time quantitative PCR and the 2(-Delta Delta C(T)) method. *Methods.* 2001;25(4):402–408. doi:10.1006/meth.2001.1262
43. Li Y, Jacox LA, Little SH, Ko CC. Orthodontic tooth movement: the biology and clinical implications. *Kaohsiung J Med Sci.* 2018;34(4):207–214. doi:10.1016/j.kjms.2018.01.007
44. Kirschneck C, Wolf M, Reicheneder C, Wahlmann U, Proff P, Roemer P. Strontium ranelate improved tooth Anchorage and reduced root resorption in orthodontic treatment of rats. *Eur J Pharmacol.* 2014;744:67–75. doi:10.1016/j.ejphar.2014.09.039
45. Liu Y, Zhang T, Zhang C, et al. Aspirin blocks orthodontic relapse via inhibition of CD4+ T lymphocytes. *J Dent Res.* 2017;96(5):586–594. doi:10.1177/0022034516685527
46. Arias OR, Marquez-Orozco MC. Aspirin, Acetaminophen, and ibuprofen: their effects on orthodontic tooth movement. *Am J Orthod Dentofacial Orthop.* 2006;130(3):364–370. doi:10.1016/j.ajodo.2004.12.027
47. Liu XC, Wang XX, Zhang LN, Yang F, Nie FJ, Zhang J. Inhibitory effects of resveratrol on orthodontic tooth movement and associated root resorption in rats. *Arch Oral Biol.* 2020;111:104642. doi:10.1016/j.archoralbio.2019.104642
48. Kirschneck C, Maurer M, Wolf M, Reicheneder C, Proff P. Regular nicotine intake increased tooth movement velocity, osteoclastogenesis and orthodontically induced dental root resorptions in a rat model. *Int J Oral Sci.* 2017;9(3):174–184. doi:10.1038/ijos.2017.34
49. Zeng MY, Tong QY. Anti-inflammation effects of sinomenine on macrophages through suppressing activated TLR4/NF- $\kappa$ B signaling pathway. *Curr Med Sci.* 2020;40(1):130–137. doi:10.1007/s11596-020-2156-6



50. Karthi M, Anbushevan GJ, Senthilkumar KP, Tamizharsi S, Raja S, Prabhakar K. NSAIDs in orthodontic tooth movement. *J Pharm Bioallied Sci.* 2012;4(Suppl 2):S304–S306. doi:10.4103/0975-7406.100280
51. Andrade I Jr, Silva TA, Silva GA, Teixeira AL, Teixeira MM. The role of tumor necrosis factor receptor type 1 in orthodontic tooth movement. *J Dent Res.* 2007;86(11):1089–1094. doi:10.1177/154405910708601113
52. Yoshimatsu M, Shibata Y, Kitaura H, et al. Experimental model of tooth movement by orthodontic force in mice and its application to tumor necrosis factor receptor-deficient mice. *J Bone Miner Metab.* 2006;24(1):20–27. doi:10.1007/s00774-005-0641-4
53. Lam J, Takeshita S, Barker JE, Kanagawa O, Ross FP, Teitelbaum SL. TNF-alpha induces osteoclastogenesis by direct stimulation of macrophages exposed to permissive levels of RANK ligand. *J Clin Invest.* 2000;106(12):1481–1488. doi:10.1172/JCI11176
54. Reitan K. Tissue behavior during orthodontic tooth movement. *Am J Orthod.* 1960;46(12):881–900. doi:10.1016/0002-9416(60)90091-9
55. de Pollak C, Arnaud E, Renier D, Marie PJ. Age-related changes in bone formation, osteoblastic cell proliferation, and differentiation during postnatal osteogenesis in human calvaria. *J Cell Biochem.* 1997;64(1):128–139.
56. Vimalraj S, Arumugam B, Miranda PJ, Selvamurugan N. Runx2: structure, function, and phosphorylation in osteoblast differentiation. *Int J Biol Macromol.* 2015;78:202–208. doi:10.1016/j.ijbiomac.2015.04.008

## Drug Design, Development and Therapy

Dovepress

### Publish your work in this journal

Drug Design, Development and Therapy is an international, peer-reviewed open-access journal that spans the spectrum of drug design and development through to clinical applications. Clinical outcomes, patient safety, and programs for the development and effective, safe, and sustained use of medicines are a feature of the journal, which has also been accepted for indexing on PubMed Central. The manuscript management system is completely online and includes a very quick and fair peer-review system, which is all easy to use. Visit <http://www.dovepress.com/testimonials.php> to read real quotes from published authors.

Submit your manuscript here: <https://www.dovepress.com/drug-design-development-and-therapy-journal>